PERGAMON

International Journal of Solids and Structures 37 (2000) 3323–3344

INTERNATIONAL JOURNAL OF SOLIDS and STRUCTURES

www.elsevier.com/locate/ijsolstr

Interactive buckling of thin-walled beam-columns with intermediate stiffeners or/and variable thickness

Zbigniew Kolakowski[a,*], Andrzej Teter[b]

[a]Technical University of Lodz, Department of Strength of Materials and Structures (K12), PL-90-924, Lodz, ul. Stefanowskiego 1/15, Poland

[b]Technical University of Lublin, Department of Applied Mechanics, PL-20-618, Lublin, ul. Nadbystrzycka 36, Poland

Received 9 July 1998; in revised form 18 January 1999

Abstract

The design of thin-walled beam-columns must take into account the overall instability and the instability of component plates in the form of local buckling. This investigation is concerned with interactive buckling of thin-walled beam-columns with central intermediate stiffeners or/and variable thickness under axial compression and a constant bending moment. The columns are assumed to be simply supported at the ends. The asymptotic expansion established by Byskov and Hutchinson (1977: Byskov, E. and Hutchinson, J. W. (1977). Mode interaction in axially stiffened cylindrical shells. AIAA J., 15(7), 941–948) is employed in the numerical calculations performed using the transition matrix method. The present paper is a continuation of the papers by Kolakowski and Teter (1995a,b: Kolakowski, Z. and Teter, A. (1995a). Interactive buckling of thin-walled closed elastic column-beams with intermediate stiffeners. Int. J. Solids Structures, 32(11), 1501–1516; Kolakowski, Z. and Teter, A. (1995b). Influence of local post-buckling behaviour on bending of thin-walled elastic beams with central intermediate stiffeners. Engineering Transactions, 43(3), 383–396) and Teter and Kolakowski (1996: Teter, A. and Kolakowski, Z. (1996). Interactive buckling of thin-walled open elastic beam-columns with intermediate stiffeners. Int. J. Solids Structures, 33(3), 315–330) where the interactive buckling of thin-walled beam-columns with central intermediate stiffeners in the first order approximation was considered. The paper's aim is to improve the study of the equilibrium path in the post-buckling behaviour of imperfect structures with regard to the second order non-linear approximation. In the solution obtained the transformation of buckling modes with an increase of the load up to the ultimate load, the effect of cross-sectional distortions and shear lag phenomenon is included. The calculations are carried out for a few beam-columns. © 2000 Elsevier Science Ltd. All rights reserved.

Keywords: Thin-walled structures; Interaction; Intermediate stiffener

* Corresponding author. Tel.: +48-42-631-2223; fax: +48-42-631-2216.
E-mail address: kola@orion.p.lodz.pl (Z. Kolakowski).

PII: S0020-7683(99)00044-X

Nomenclature

a_{jkr}, b_{rrrr}	three- and four-index coefficients in the non-linear equilibrium Eq. (11) (Byskov and Hutchinson, 1977)
$\bar{a}_i^{(j)}$, $\bar{b}_i^{(j)}$, $\bar{c}_i^{(j)}$, $\bar{d}_i^{(j)}$, $\bar{e}_i^{(j)}$, $\bar{f}_i^{(j)}$, $\bar{g}_i^{(j)}$, $\bar{h}_i^{(j)}$	orthogonal functions for the first order approximation (Eq. (6))
$\hat{a}_i^{(jj)}$, $\hat{b}_i^{(jj)}$, $\hat{c}_i^{(jj)}$, $\hat{d}_i^{(jj)}$, $\hat{e}_i^{(jj)}$, $\hat{f}_i^{(jj)}$, $\hat{g}_i^{(jj)}$, $\hat{h}_i^{(jj)}$	orthogonal functions for the second order approximation (Eq. (8))
b_i	width of the i-th wall of the column
h_i	thickness of the i-th wall of the column
j	number of the mode
J	number of the interacting mode
l	length of the column
m	number of axial half-waves of the mode
M_{ix}, M_{iy}, M_{ixy}	bending moment resultants for the i-th wall
$\bar{\mathbf{N}}$	force field
N_{ix}, N_{iy}, N_{ixy}	in-plane resultants for the i-th wall
$N_{\mathrm{ix}}^{(0)}$	pre-buckling in-plane stress for the i-th wall
$\bar{\mathbf{U}}$	displacement field
u_i, v_i, w_i	displacement components of the middle surface of the i-th wall
Δ_i	measure of the applied pressure
ϵ_{ix}, ϵ_{iy}, ϵ_{ixy}	strain tensor components for the middle surface of the i-th wall
κ_{ix}, κ_{iy}, κ_{ixy}	curvature modifications and torsions of the middle surface of the i-th wall
λ	scalar load parameter
λ_j	value of at the bifurcation mode number j
λ_{s}	maximum value of λ for the imperfect column
$\sigma_j^* = \sigma_j 10^3/\mathrm{E}$	dimensionless stress of the j-th mode
σ_{m}^*	$\min(\sigma_1^*, \sigma_2^*, \sigma_3^*, \ldots \sigma_J^*)$
σ_{s}^*	limit dimensionless stress for imperfect column (load carrying capacity)
ζ_j	amplitude buckling mode number j
ζ_j	imperfection amplitude corresponding to ζ_j
ξ_i	x_i/b_i nondimensional coordinate

1. Introduction

Thin-walled structures consisting of plate elements and having a number of buckling modes differ from one another both in quantitative (e.g. by the number of half-waves) and in qualitative (e.g. by global and local buckling) respects.

Local buckling is the major feature to be taken into account in the design of thin-walled sections. Thin-walled structures, especially columns and beams, may have many buckling modes and are able to sustain load after local buckling. The local buckles cause reduction in the stiffness of a section and, consequently, lower the load carrying capacity relative to a non-locally buckled section. The determination of their load carrying capacity requires consideration of the modal interaction of buckling modes and imperfections in the non-linear analysis of stability. The problem of the interaction of the global mode with the local ones is of great significance.

Intermediate stiffeners are widely used in many types of metal structures. These stiffeners carry a portion of loads and subdivide the plate element into smaller sub-elements, thus increasing considerably the load-carrying capacity. The shape, size and position of intermediate stiffeners in thin-walled structures exert a strong influence on the stability and postbuckling behaviour of the thin-walled structures. The importance of the minimum rigidity of the intermediate stiffeners required to restrict buckling to the plate elements was studied e.g. by Timoshenko (1921), Cox and Riddell (1949), Desmond (1977), Höglund (1978), Konig (1978).

The test specimens, experimental works and comparisons made with design rules of plates and open cross-section structures were detailed by Hoon et al. (1993), Bernard et al. (1993). Mathematical models tend to higher precision and closer approximation of real structures, which enables one to analyse more and more exactly the phenomena occurring during and after the loss of stability.

The concept of interactive buckling involves the general asymptotic non-linear theory of stability. The theory is based on asymptotic expansions of the post-buckling path and is capable of considering simultaneous or nearly simultaneous buckling modes (Byskov and Hutchinson, 1977).

As far as the first order approximation in concerned, Koiter and van der Neut (1980) have proposed a technique in which the interaction of an overall mode with two local modes having the same wavelength (i.e. three-mode approach) has been considered. The fundamental local mode is henceforth called 'primary' and the nontrivial higher mode (having the same wavelength as the 'primary' one), corresponding to the mode triggered by the overall long wave mode, is called 'secondary'. In the energy expression for the first order non-linear approximation the coefficients of the cubic terms $\zeta_1\zeta_2^2$, $\zeta_1\zeta_3^2$ and $\zeta_1\zeta_2\zeta_3$ (where ζ_j is the amplitude of j-th buckling mode and the index is: 1 for the global mode, 2 for the primary local buckling mode and 3 for the secondary local mode) are the key terms governing the interaction.

Consideration of displacements and load components in the middle surface of walls within the first order approximation as well as precise geometrical relationships enabled the analysis of all possible buckling modes including a mixed buckling mode (for a more detailed analysis see papers by Camotim and Prola, 1996; Dubina, 1996; Teter and Kolakowski, 1996; Kolakowski et al., 1997). In thin-walled structures of open cross-sections, owning to their low rigidity, it is necessary to consider distortional deformations. The above factors have even led to consideration of an interaction of a few modes—two global and some local ones.

If the analysis of the stability problem of thin-walled structures is restricted to the first order approximation, the imperfection sensitivity can only be obtained. The determination of the post-buckling equilibrium path requires the second order approximation to be taken into account. The structures where the local buckling precedes the global one ($\lambda_2 > \lambda_1$ i.e. $\sigma_2^* > \sigma_1^*$) are widely used because these structures can carry a load higher than that referring to the bifurcation value of the local buckling.

Therefore, it is necessary to consider the second order approximation, that is the fourth order components of the potential energy (coefficients of the terms $\zeta_j^2\zeta_k^2$). In general, the stability analysis with regard to the second non-linear approximation requires the solution of boundary value problems: for the second order global, local and mixed modes. However, in the case when $\lambda_2 > \lambda_1$ the most significant are local second order modes. The second order global mode for a beam-bar model of the column is zero and in the case of an exact solution it is of little importance in more instances.

In the case of the mixed field of the second order, the left-hand side of the equilibrium equation is the same as in the first order approximation (in eigenvalues problem) and the load parameter λ is very often assumed to be $\lambda = \min(\lambda_1, \lambda_2, \ldots \lambda_J)$. The right-hand side of the equilibrium equation can be treated as a loading term proportional to the displacements corresponding to the global buckling mode ($m = 1$), to the displacements referring to the local buckling modes ($m \gg 1$) and to the factors standing by the arguments ($m - 1$) or ($m + 1$) of respective trigonometric functions (Sridharan and Ali, 1986; Sridharan and Peng, 1989; Kasagi and Sridharan, 1995). On the other hand, consideration of the second-order approximation makes sense only when $\lambda_2 > \lambda_1$. In view of this and in the case of $\lambda_2 > \lambda_r$ ($r \geq 3, \ldots J$) it is practically assumed that $\lambda = \lambda_2$. The eigenvalues of the mixed second-order field for global and local modes are nearly the same as the eigenvalue of the local buckling mode, $m \gg 1$. Therefore, both eigenvalue problems are almost identical. The system of equilibrium equations for second-order mixed modes with non-zero right-hand members is wrongly conditioned from the numerical point of view, since a characteristic determinant for such a system is nearly zero.

On the other hand, an omission of the second order mixed mode is possible owing to the fact that three-mode approach has been already included in the analysis. The admissibility of neglecting the mixed mode was shown by Koiter (1976), Sridharan and Peng (1989).

The equations for local modes in the second approximation depend not only on the respective first order local modes, but, regarding the orthogonality conditions, also on the considered first order modes. Therefore, none of the local second order modes obtained with allowance for interactive buckling is identical with the mode obtained according to the theory of single-mode buckling (an uncoupled buckling), where the condition of orthogonality in relation to the global mode is not binding.

A more comprehensive review of the literature concerning the interactive buckling analysis of an isotropic structure can be found in papers by Koiter and Pignataro (1976), Manevich (1985, 1988), Moellmann and Goltermann (1989), Pignataro et al. (1985, 1987a,b), Sridharan and Ali (1985, 1986), Krolak (1990), Kolakowski (1987a, 1989a–c, 1993a,b).

In the present paper which is a continuation of the papers devoted to the first order approximation written by Kolakowski and Teter (1995a) and Teter and Kolakowski (1996), an analysis of the load carrying capacity of beam-columns in the second non-linear approximation considering only local second order modes is undertaken. Thin-walled structures with the intermediate stiffeners or/and variable thickness in the elastic range being under axial compression and a bending moment are examined on the basis of Byskov and Hutchinson's method and the co-operation between all the walls of structures being taken into account is shown. The study is based on the numerical method of the transition matrix (Unger, 1969; Bilstein, 1974) using Godunov's orthogonalization (Biderman, 1977). The most important advantage of this method is that it enables us to describe a complete range of behaviour of the thin-walled structures from all global (flexural, flexural–torsional, lateral, distortional and their combinations) to local stability. In the solution obtained, the effects of interaction of certain modes having the same wavelength, the transformation of buckling modes with the increase of load, the shear lag phenomenon and also the effect of cross-sectional distortions are included. The distortion instability of beam-columns is investigated using non-linear theory.

2. Structural problem

The long thin-walled prismatic beam-columns of length l, composed of plane, rectangular plate segments interconnected along longitudinal edges, simply supported at both ends, are considered. The cross-section of this structure composed of several plates, as well as the local Cartesian co-ordinate systems, are presented in Fig. 1.

A plate model is adopted for the beam-columns. For the *i*-th plate component precise geometrical relationships are assumed in order to enable the consideration of both out-of-plane and in-plane bending of each plate:

$$\epsilon_{ix} = u_{i,\,x} + \frac{1}{2}(w_{i,\,x}^2 + v_{i,\,x}^2),$$

$$\epsilon_{iy} = v_{i,\,y} + \frac{1}{2}(w_{i,\,y}^2 + u_{i,\,y}^2),$$

$$2\epsilon_{ixy} = \gamma_{ixy} = u_{i,\,y} + v_{i,\,x} + w_{i,\,x}w_{i,\,y},$$

$$\kappa_{ix} = -w_{i,\,xx}, \quad \kappa_{iy} = -w_{i,\,yy}, \quad \kappa_{ixy} = -w_{i,\,xy}. \tag{1}$$

The differential equilibrium equations resulting from the virtual work principle and corresponding to expressions (1) for the *i*-th plate can be written as follows:

$$N_{ix,\,x} + N_{ixy,\,y} + (N_{iy}u_{i,\,y})_{,\,y} = 0,$$

$$N_{ixy,\,x} + N_{iy,\,y} + (N_{ix}v_{i,\,x})_{,\,x} = 0,$$

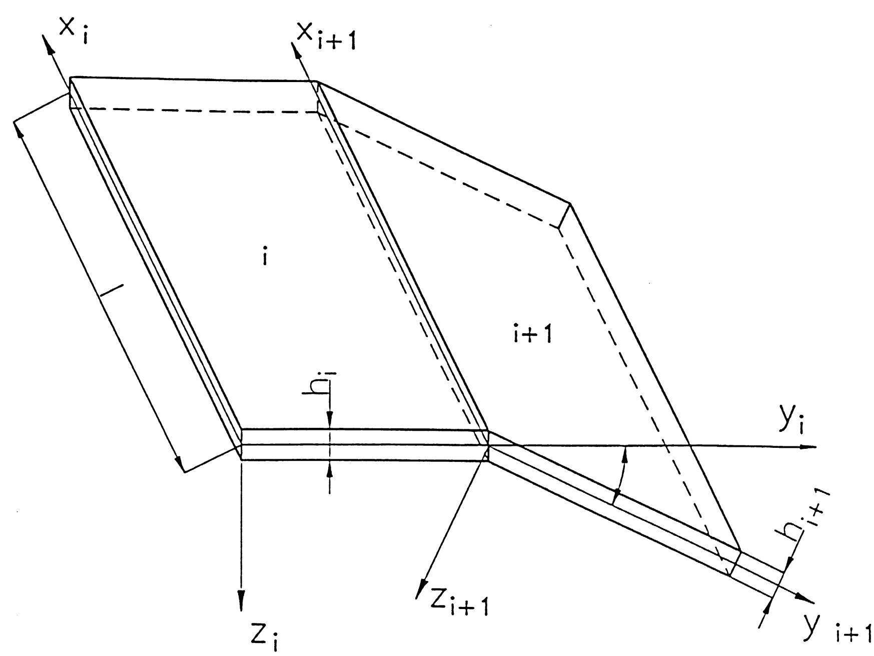

Fig. 1. Prismatic plate structure and the local co-ordinate system.

$$(N_{ix}w_{i,\,x})_{,\,x} + (N_{iy}w_{i,\,y})_{,\,y} + (N_{ixy}w_{i,\,x})_{,\,y} + (N_{ixy}w_{i,\,y})_{,\,x} + M_{ix,\,xx} + M_{iy,\,yy} + 2M_{ixy,\,xy} = 0. \tag{2}$$

The non-linear problem is solved by Byskov and Hutchinson asymptotic method (1977). The displacement fields $\bar{\mathbf{U}}$, and the sectional force fields, $\bar{\mathbf{N}}$, are expanded in power series in the buckling mode amplitudes, ζ_j (ζ_j is the amplitude of the j-th buckling mode divided by thickness of the first component plate, h_1):

$$\bar{\mathbf{U}} = \lambda \bar{U}_i^{(0)} + \zeta_j \bar{U}_i^{(j)} + \zeta_j \zeta_k \bar{U}_i^{(jk)} + \cdots$$

$$\bar{\mathbf{N}} = \lambda \bar{N}_i^{(0)} + \zeta_j \bar{N}_i^{(j)} + \zeta_j \zeta_k \bar{N}_i^{(jk)} + \cdots \tag{3}$$

where the pre-buckling fields are $\bar{U}_i^{(0)}$, $\bar{N}_i^{(0)}$, the buckling mode fields are $\bar{U}_i^{(j)}$, $\bar{N}_i^{(j)}$ and the post-buckling fields $\bar{U}_i^{(jk)}$, $\bar{N}_i^{(jk)}$. The range of indices is $[1, J]$ where J is the number of interacting modes.

By substituting expansion (3) into equations of equilibrium (2), junction conditions (12) and boundary conditions (14), the boundary value problems of zero, first and second order can be obtained. The zero approximation describes the pre-buckling state while the first approximation, that is the linear problem of stability, enables us to determine the critical loads of global and local value and their buckling modes. This question can be reduced to a homogeneous system of differential equilibrium equations. The second order boundary problem can be reduced to a linear system of non-homogeneous equations, whose right-hand sides depend on the first order displacement and force fields.

3. Solution of the problem

The plates with linearly varying pre-buckling stresses along their widths are divided into several strips under uniformly distributed compressive (tensile) stresses (Fig. 2). Instead of the finite strip method, the exact transition matrix method is used in this case.

The pre-buckling solution of the i-th plate consisting of homogeneous fields is assumed to be:

$$u_i^{(0)} = \left(\frac{l}{2} - x_i\right)\Delta_i,$$

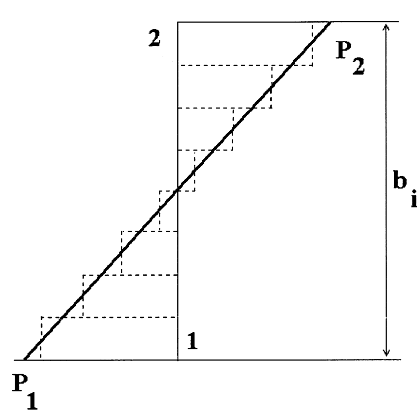

Fig. 2. Discretization of a linear distribution of stresses by means of finite strips.

$$v_i^{(0)} = \nu_i y_i \Delta_i,$$

$$w_i^{(0)} = 0, \tag{4}$$

so:

$$N_{ix}^{(0)} = -E_i h_i \Delta_i \quad N_{iy}^{(0)} = N_{ixy}^{(0)} = 0 \tag{5}$$

where Δ_i is the actual loading. This loading is specified as the product of a unit loading system and a scalar load factor Δ_i.

The omission of the displacements of the fundamental state implies that we ignore the difference between configuration of the undeformed state and the fundamental state and we may consequently regard the previously defined displacements $u_i^{(0)}$, $v_i^{(0)}$ as the additional ones from the fundamental state to the adjacent state.

Numerical aspects of the problem being solved for the first order fields (Kolakowski and Teter, 1995a), resulted in an introduction of the following new orthogonal functions in the sense of boundary conditions for two longitudinal edges (see Appendix B):

$$\bar{a}_i^{(j)} = v_{i,\chi}^{(j)} + \nu_i u_{i,\xi}^{(j)},$$

$$\bar{b}_i^{(j)} = 0.5(1-\nu_i)(u_{i,\chi}^{(j)} + v_{i,\xi}^{(j)}),$$

$$\bar{c}_i^{(j)} = u_i^{(j)},$$

$$\bar{d}_i^{(j)} = v_i^{(j)},$$

$$\bar{e}_i^{(j)} = w_i^{(j)},$$

$$\bar{f}_i^{(j)} = w_{i,\chi}^{(j)},$$

$$\bar{g}_i^{(j)} = w_{i,\chi\chi}^{(j)} + \nu_i w_{i,\xi\xi}^{(j)},$$

$$\bar{h}_i^{(j)} = w_{i,\chi\chi\chi}^{(j)} + (2-\nu_i) w_{i,\xi\xi\chi}^{(j)}. \tag{6}$$

The boundary conditions (14) permit the first order solution to be written as:

$$\bar{a}_i^{(j)} = \bar{A}_i^{(j)}(\chi_i) \sin \frac{m\pi b_i}{l} \xi_i,$$

$$\bar{b}_i^{(j)} = \bar{B}_i^{(j)}(\chi_i) \cos \frac{m\pi b_i}{l} \xi_i,$$

$$\bar{c}_i^{(j)} = \bar{C}_i^{(j)}(\chi_i) \cos \frac{m\pi b_i}{l} \xi_i,$$

$$\bar{d}_i^{(j)} = \bar{D}_i^{(j)}(\chi_i)\sin\frac{m\pi b_i}{l}\xi_i,$$

$$\bar{e}_i^{(j)} = \bar{E}_i^{(j)}(\chi_i)\sin\frac{m\pi b_i}{l}\xi_i,$$

$$\bar{f}_i^{(j)} = \bar{F}_i^{(j)}(\chi_i)\sin\frac{m\pi b_i}{l}\xi_i,$$

$$\bar{g}_i^{(j)} = \bar{G}_i^{(j)}(\chi_i)\sin\frac{m\pi b_i}{l}\xi_i,$$

$$\bar{h}_i^{(j)} = \bar{H}_i^{(j)}(\chi_i)\sin\frac{m\pi b_i}{l}\xi_i, \tag{7}$$

where $\bar{A}_i^{(j)}$, $\bar{B}_i^{(j)}$, $\bar{C}_i^{(j)}$, $\bar{D}_i^{(j)}$, $\bar{E}_i^{(j)}$, $\bar{F}_i^{(j)}$, $\bar{G}_i^{(j)}$, $\bar{H}_i^{(j)}$ (with the m-th harmonic) are initially unknown functions defined by the modified numerical transition matrix method. The system of the ordinary differential equilibrium Eqs. (2) for the first order approximation is solved by the modified transition matrix method in which the state vector of the final edge is derived from the state vector of the initial edge by numerical integration of the differential equations in the $\chi_i = y_i/b_i$-direction using the Runge–Kutta formulae by means of the Godunov orthogonalization method (Biderman, 1977).

The global buckling mode occurs at $m = 1$ and the local modes at $m \gg 1$ (with $b_i \ll l$).

Analogously to the introduction of the orthogonal functions (6), the adopted boundary conditions (14) require an introduction of new functions for the second order fields:

$$\hat{a}_i^{(jj)} = v_{i,\chi}^{(jj)} + \nu_i u_{i,\xi}^{(jj)},$$

$$\hat{b}_i^{(jj)} = 0.5(1-\nu_i)(u_{i,\chi}^{(jj)} + v_{i,\xi}^{(jj)}),$$

$$\hat{c}_i^{(jj)} = u_i^{(jj)},$$

$$\hat{d}_i^{(jj)} = v_i^{(jj)},$$

$$\hat{e}_i^{(jj)} = w_i^{(jj)},$$

$$\hat{f}_i^{(jj)} = w_{i,\chi}^{(jj)},$$

$$\hat{g}_i^{(jj)} = w_{i,\chi\chi}^{(jj)} + \nu_i w_{i,\xi\xi}^{(jj)},$$

$$\hat{h}_i^{(jj)} = w_{i,\chi\chi\chi}^{(jj)} + (2-\nu_i) w_{i,\xi\xi\chi}^{(jj)}. \tag{8}$$

The main difference in the presented method of solution consists in an introduction of the orthogonal force and displacement functions in the first and second order approximation in contradistinction to paper by Kolakowski (1993a,b) where only new non-orthogonal functions were introduced for the second order solution.

The easiness of satisfying the orthogonality conditions allows the second order fields to be formulated as follows:

$$\hat{a}_i^{(jj)} = \sum_n \hat{A}_{in}^{(jj)}(\chi_i) \sin \frac{n\pi b_i}{l}\xi_i + A_i^{*(jj)},$$

$$\hat{b}_i^{(jj)} = \sum_n \hat{B}_{in}^{(jj)}(\chi_i) \cos \frac{n\pi b_i}{l}\xi_i,$$

$$\hat{c}_i^{(jj)} = \sum_n \hat{C}_{in}^{(jj)}(\chi_i) \cos \frac{n\pi b_i}{l}\xi_i + C_i^{*(jj)}\left(\frac{l}{2} - b_i\xi_i\right),$$

$$\hat{d}_i^{(jj)} = \sum_n \hat{D}_{in}^{(jj)}(\chi_i) \sin \frac{n\pi b_i}{l}\xi_i,$$

$$\hat{e}_i^{(jj)} = \sum_n \hat{E}_{in}^{(jj)}(\chi_i) \sin \frac{n\pi b_i}{l}\xi_i,$$

$$\hat{f}_i^{(jj)} = \sum_n \hat{F}_{in}^{(jj)}(\chi_i) \sin \frac{n\pi b_i}{l}\xi_i,$$

$$\hat{g}_i^{(jj)} = \sum_n \hat{G}_{in}^{(jj)}(\chi_i) \sin \frac{n\pi b_i}{l}\xi_i,$$

$$\hat{h}_i^{(jj)} = \sum_n \hat{H}_{in}^{(jj)}(\chi_i) \sin \frac{n\pi b_i}{l}\xi_i, \tag{9}$$

where

$$A_i^{*(jj)} = -\nu_i b_i C_i^{*(jj)}$$

$$C_i^{*(jj)} = \frac{\int_0^1 \left\{ \left(\frac{m\pi b_i}{l}\right)^2 [\bar{D}_i^{(j)^2} + \bar{E}_i^{(j)^2}] + \frac{2}{1-\nu_i}\left[B_i^{(j)} - \left(\frac{m\pi b_i}{l}\right)\bar{D}_i^{(j)}\right]^2 \right\} \mathrm{d}\chi_i}{2b_i^2 \int_0^1 \mathrm{d}\chi_i}. \tag{10}$$

$\hat{A}_{in}^{(jj)}$, $\hat{B}_{in}^{(jj)}$, $\hat{C}_{in}^{(jj)}$, $\hat{D}_{in}^{(jj)}$, $\hat{E}_{in}^{(jj)}$, $\hat{F}_{in}^{(jj)}$, $\hat{G}_{in}^{(jj)}$, $\hat{H}_{in}^{(jj)}$ are unknown functions that shall be determined by the method of transition matrix in the same way as the first order fields.

The coefficients $C_i^{*(jj)}$ and $A_i^{*(jj)}$ have been found from condition (14) and from Eqs. (8), respectively.

Owing to the correction factors $A_i^{*(jj)}$, $C_i^{*(jj)}$ introduced into (9), the additional longitudinal compression caused by the influence of the first order displacement field upon the second order approximation can be reduced to zero at both ends. The above factors allow to satisfy identical boundary conditions (14) both for the first and the second order approximation.

The Poisson's effect is, like in the case of the first approximation, neglected at both ends and is taken into account inside the plate areas.

Taking into account the components of membrane forces and displacements within the first order approximation allows to consider shear-lag phenomenon and the distortions of cross-sections, whereas the assumption of a non-zero deflection within the second order approximation accounts for the transformation of displacement and force fields with the increase of loading that is disregarded in most works.

At the point where the load parameter λ reaches its maximum value λ_s for the imperfect structure (secondary bifurcation or limit points), the Jacobian of the non-linear system of equations (Byskov and Hutchinson, 1977):

$$\left(1-\frac{\lambda}{\lambda_r}\right)\zeta_r + a_{jkr}\zeta_j\zeta_k + b_{rrrr}\zeta_r^3 + \cdots = \frac{\lambda}{\lambda_r}\bar{\zeta}_r \quad \text{at} \quad r = 1, 2, \ldots J \tag{11}$$

is equal to zero.

Expressions for a_{jkr}, b_{rrrr} are calculated by known formulae (Byskov and Hutchinson, 1977). The formulae for the postbuckling coefficients a_{jkr} depend only on the buckling modes, whereas the coefficients b_{rrrr} also depend on the second order field.

The result of integration along $x_i = \xi_i b_i$ indicates that the post-buckling coefficients a_{jkr} are zero when the sum of the wave numbers associated with the three modes $(m_j + m_k + m_r)$ is even, while the coefficients b_{rrrr} are non-zero.

Considering only linear initial imperfections (determined by the shape of J coupled buckling modes) and components of displacement and force fields for the first order allows us, to some extent, to account for the residual stresses. However the residual stresses are not assumed in advance and this approach can only be treated as an attempt to consider their most unfavourable distribution. For a rather extensive discussion see papers by Pignataro and Luongo (1987a,b).

4. Analysis of results

The numerical analysis concerning the second order local fields in thin-walled structures depends on the coefficients determining the nature of the post-buckling behaviour as functions of structural parameters and the influence of these coefficients upon equilibrium branches and the load carrying capacity. The accuracy of trigonometric series convergence was found sufficient for practical purposes with up to 50 non-zero harmonics considered (n = 1, 3, 5, ..., 99). This ensured obtaining the accuracy of displacement and stress fields below 0.1%.

In all analysed cases the post-buckling coefficients b_{rrrr} are positive.

With regard to 'exact' continuity conditions at longitudinal sides of the structure for $\varphi_{i,i+1} \neq 0$ as early as in the first order approximation, non-zero displacement components appear. If the simplified boundary conditions are adopted for longitudinal sides, the above component is very often omitted.

The character of the second order field determining the post-buckling behaviour for uncoupled local buckling modes varies, subject to the mode of the first order buckling in question. The second order stresses are the sums of two components $\sigma^{(jj)} = \sigma_1^{(jj)} + \sigma_2^{(jj)}$, where $\sigma_1^{(jj)}$ stands for the stress corresponding to the first order displacements, $\sigma_2^{(jj)}$ represents stresses found on the basis of the second order displacement field (for a more detailed analysis see papers by Kolakowski, 1993a,b).

The orthogonality condition of global and local first order modes relative to the local second order modes implies that in the latter case amplitudes should be changed for $n = 1$ and $n = m$ if m is an odd number of half-waves in the longitudinal direction. This results from the adoption of series form (9) for the second order field and from the fact that odd n values are summed.

The largest contribution to the second order fields is made by harmonics for low values of n ($n = 1, 3, 5$) and for n close to $2 \ m$. Hence the amplitude corrections at $n = 1$ and $n =$ m (where $m = 3, 5, 7$), which is characteristic for example, of open-section columns, compressed stiffened plates, may lead to a significant change in the value of b_{rrrr} ($r > 1$) coefficients.

The second order field was determined along with the coefficients b_{rrrr} corresponding to the second order approximation for $\lambda = \min(\lambda_1, \lambda_{2,} \ldots \lambda_J)$.

The long thin-walled prismatic beam-columns of a square cross-section with variable thickness (Fig. 3(a)), with corners bevelled at the angle of 45 (Fig. 3(b) and (c)) reinforced with C-shaped central intermediate stiffeners (Fig. 3(d)) have been performed. The bevelled corners and intermediate stiffeners are built of plates whose width is b_s. Detailed numerical calculations have been carried out for a few cross-sectional reinforcements of thin-walled beam-columns subject to uniform and eccentric compression.

In the pre-buckling state the beam-column is subjected to linearly variable stresses caused by an axial force and a bending moment which are dealt with as external loads. The load distribution can be described with the ratio of stress $p_i(y)$ at the point i of the cross-section to the greatest compressive stress, $p_{\max} = p_1$ applied to the top flange (Fig. 3). In the presented paper the load distribution is defined by the ratio of stresses in the bottom flange (point 2) to maximum stresses in the top flange (point 1), $\kappa = p_2/p_1 = p_2/p_{\max}$. The stress p_i is considered positive if it is a compressive stress. In order to compare load capacities of different cross-sections (Fig. 3(a)–(d)), identical distributions of external stress are assumed; this implies a change in the values of a compressive force and a bending moment.

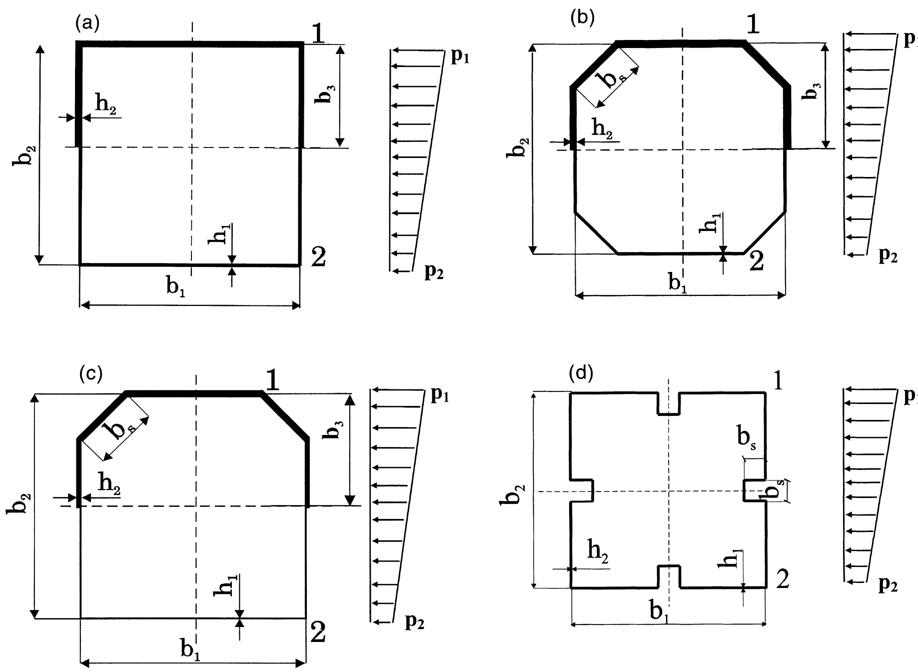

Fig. 3. Types of closed cross-section considered.

The calculations are carried out for a beam-column of the following geometrical dimensions (Fig. 3(a)–(c)):

$$b_1/b_3 = 2.0; \quad b_1/b_2 = 1.0; \quad h_1/h_2 = 1.5; \quad l/b_2 = 8; \quad b_1/h_1 = 100; \quad \nu = 0.3$$

and for the bevelled corners:

$$b_s/h_1 = \{0, 9, 18, 27\}.$$

Figs. 4–7 present the dimensionless critical stress σ_r^*, instead of the load parameter λ_r, as a function of the number of half-waves, m, for the beam-column subjected to the uniform ($\kappa = 1$) and eccentric ($\kappa = 0$) compression and for the above values of b_s/h_1. As a comparison, the results are shown as obtained for a 'smooth' square column with variable thickness (i.e. for $b_s/h_1 = 0$, in Figs. 4(0)–7(0)).

While analysing the values of critical loads, it has been found that in the case of the axial compression ($k = 1$) a change in the wall thickness and bevelling two corners only is purposeless (Fig. 3(c)) as the values of critical stresses for local and global buckling modes do not change practically, independently of the size of bevelling (Fig. 5). In this case, the broadest of the plates creating a column (i.e. the bottom flange) is subjected to buckling, and other plates follow it. Thus, a modification in the cross-section by means of bevelling the remaining corners is necessary (Fig. 3(b)) in order to increase rigidity of the component plates. In this case a desirable increase in the critical stresses corresponding to the local buckling (Fig. 4) can be observed. In the case of a column with bevelled corners with the reinforcement $b_s/h_1 = 27$, the lowest critical stresses corresponding to the local buckling increase three times. An influence of the size of corner bevelling for the assumed type of the cross-section and load does not cause in practice an increase in global stresses owing to small changes in the moment of inertia of the cross-section.

A modification of the square cross-section (Fig. 3(a)) accomplished by corner bevelling (Fig. 3(b) and (c)) results in the expected increase in the local critical stress value owing to the growth of flexural rigidity of the component plates, and in a slight increase in global critical stress value (up to about 10%) as has been mentioned above.

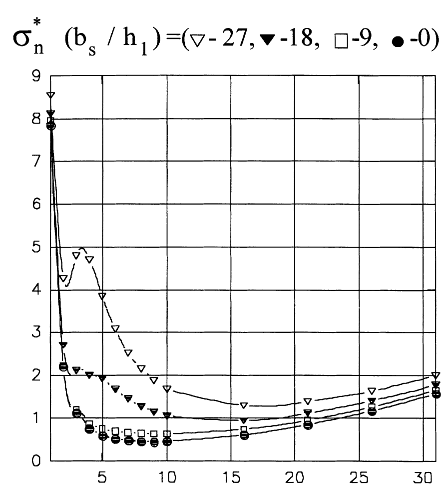

Fig. 4. Dimensionless stress σ_r^* vs the number of half-waves m for uniform compression column ($\kappa = 1$) with cross-section presented in Fig. 3(b).

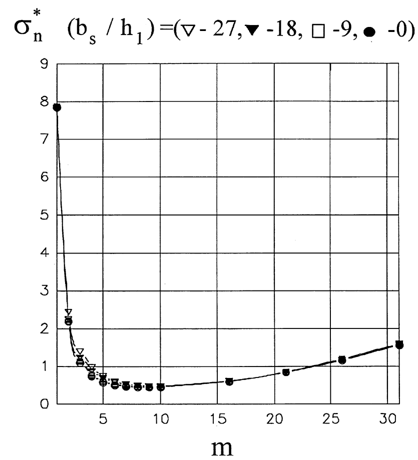

Fig. 5. Dimensionless stress σ_r^* vs the number of half-waves m for uniform compression column ($\kappa = 1$) with cross-section presented in Fig. 3(c).

The assumption of the plate model of a beam-column has allowed for an analysis of the effect of the eccentricity of the applied force on the global stability, which is impossible in the case the beam model is assumed.

While investigating critical states of beam-columns subjected to the eccentric compression ($\kappa = 0$), it has been found that a change in the wall thickness and bevelling two corners only (Fig. 3(c)) results in a desirable increase in the stresses corresponding to the local buckling (Fig. 7). An increase in the eccentricity of the compressive force is followed by an increase in the stability coefficient of the webs and the bottom flange, which in turn, causes the global and the local critical load to increase twice. In this case, for the reinforcement $b_s/h_1 = 27$, the lowest critical stresses corresponding to the local buckling increase three times. An application of additional corner bevelling (Fig. 3(b)) is not as much purposeful in this case, because it does not exert in practice any influence on the value of the global and the local critical load (cf. Figs. 6 and 7).

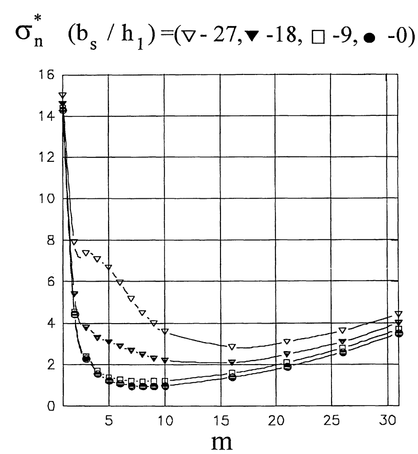

Fig. 6. Dimensionless stress σ_r^* vs the number of half-waves m for compressed eccentrically column ($\kappa = 0$) with cross-section presented in Fig. 3(b).

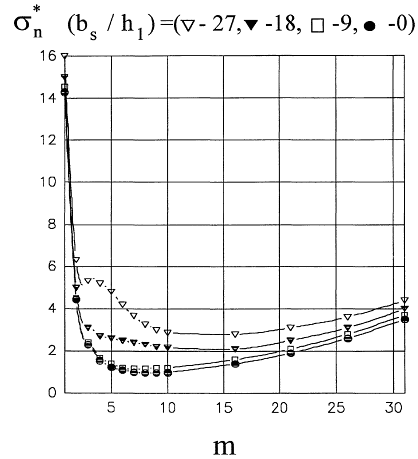

Fig. 7. Dimensionless stress σ_r^* vs the number of half-waves m for compressed eccentrically column ($\kappa = 0$) with cross-section presented in Fig. 3(c).

In order to determine the maximum value of the load (the so-called limit load capacity) of a real structure, it is necessary to take into account an interaction of different buckling modes. In the analysis of an interaction of buckling modes of such a structure, one should consider the global buckling mode, the primary and the secondary local buckling mode. Detailed numerical calculations have been carried out for the beam-columns analysed (Fig. 3(a)–(c)), characterized by the following imperfection values: $\bar{\zeta}_1 = | 1.0 |$, $\bar{\zeta}_2 = | 0.2 |$, $\bar{\zeta}_3 = 0.0$ where the index is: 1—for the global mode, 2—for the primary local buckling mode, and 3—for the secondary local buckling mode, respectively.

An assumption of the global imperfection takes into account the global pre-buckling bending of the beam-column.

In Tables 1–3 the values of the dimensionless critical stresses σ_r^*, along with the number of half-waves m (in brackets) and the dimensionless limit load capacity values $\sigma_s^* = \sigma_s 10^3/E$ referred to the minimum value of the critical stresses $\sigma_m^* = \min(\sigma_1^*, \sigma_2^*, \sigma_3^*)$ for the columns under consideration (Fig. 3(a)–(c)) are presented.

In each case the signs of the imperfections have been chosen in the most unfavourable fashion, i.e. so that σ_s^* would assume its minimum value (see Manevich, 1988; Kolakowski, 1987a,b, 1989a, 1989c, for a more detailed discussion).

The local mode imperfections always promote an interaction between the local modes and the global mode.

In the cases being analysed, the value of the global Euler critical load exceeds the lowest local critical load: for the column shown in Fig. 3(a) and (b)—a few times, and for the column depicted in Fig. 3(a) and (c)—even more than 10 times. Taking into account the second order approximation causes that the

Table 1
Load-carrying capacity σ_s^*/σ_m^* for beam-column with cross-section presented in Fig. 3(a) at imperfections $\bar{\zeta}_1 = | 1.0 |$, $\bar{\zeta}_2 = | 0.2 |$, $\bar{\zeta}_3 = 0.0$

	b_s/h_1	κ	σ_1^*	σ_2^*	σ_3^*	σ_s^*/σ_m^*
1	0	1	7.862(1)	0.4553(9)	0.7561(9)	1.6670
2	0	0	14.290(1)	0.9713(8)	1.9175(8)	1.5073

Table 2
Load-carrying σ_s^*/σ_m^* capacity for beam-column with cross-section presented in Fig. 3(b) at imperfections $\bar{\zeta}_1 = \mid 1.0 \mid$, $\bar{\zeta}_2 = \mid 0.2 \mid$, $\bar{\zeta}_3 = 0.0$

	b_s/h_1	κ	σ_1^*	σ_2^*	σ_3^*	σ_s^*/σ_m^*
1	27	1	8.5501(1)	1.2890(16)	1.9389(16)	1.5266
2	18	1	8.1226(1)	0.9280(14)	1.3870(14)	1.5255
3	9	1	7.9635(1)	0.6305(10)	0.9170(10)	1.5439
4	27	0	14.9983(1)	2.8545(16)	3.9821(16)	1.5101
5	18	0	14.5932(1)	2.0216(14)	2.8385(14)	1.5284
6	9	0	14.4075(1)	1.2122(8)	2.3792(8)	1.5264

theoretical limit load capacity increases one and half times in comparison with the minimum value of the local load. In the case the analysis limitation to the first order approximation is not sufficient and can only be treated as the lower bound estimation of the load carrying capacity.

In the case of the eccentric compression the global stress values, σ_r^*, are significantly higher than under the uniform compression while the limit stress values, σ_s^*/σ_m^* are lower (compare cases 1–4, 2–5, 3–6 in Tables 2 and 3, respectively, and cases 1 and 2 in Table 1). This means that the imperfection sensitivity increases together with the eccentricity of the compressive force.

The calculations have confirmed that in the case when the value of the global load exceeds the value of the local load, it is possible to reach the limit load capacity higher than the minimum value of the local load for a moderately low value of the imperfection.

Taking into account the second order approximation enables us to determine the limit load capacity of the structure in an elastic range. An assumption of one of the 'engineering' hypotheses of the load carrying capacity allows for determination of the limit load for an elastic–plastic range (see the paper by Manevich and Kolakowski, 1996; Kolakowski and Teter, 1995b).

The calculations are carried out for a beam-column of a closed cross-section reinforced with C-shaped central intermediate stiffeners of the following constant geometrical dimensions (Fig. 3(d)):

$$b_1/b_2 = 1.0; \quad h_1/h_2 = 1.0; \quad l/b_2 = 20; \quad b_1/h_1 = 100; \quad \nu = 0.3.$$

Central intermediate stiffeners are modelled with plates, their dimensions being:

$$b_s/h_1 = \{0, 8\}.$$

The cases of the uniform—$\kappa = 1$ (Fig. 8(a)) and eccentric—$\kappa = 0$ (Fig. 8(b)) compression are analysed.

The introduction of central intermediate stiffeners increases the flexural rigidity of plate elements and,

Table 3
Load-carrying capacity σ_s^*/σ_m^* for beam-column with cross-section presented in Fig 3(c) at imperfections $\bar{\zeta}_1 = \mid 1.0 \mid$, $\bar{\zeta}_2 = \mid 0.2 \mid$, $\bar{\zeta}_3 = 0.0$

	b_s/h_1	κ	σ_1^*	σ_2^*	σ_3^*	σ_s^*/σ_m^*
1	27	1	7.7853(1)	0.4782(10)	1.2204(10)	2.5514
2	18	1	7.8355(1)	0.4735(10)	1.0452(10)	2.2236
3	9	1	7.8724(1)	0.4625(9)	0.8435(9)	1.8346
4	27	0	16.3150(1)	2.7087(13)	3.0560(13)	1.1253
5	18	0	15.2128(1)	2.0219(14)	2.3446(14)	1.3091
6	9	0	14.5589(1)	1.1644(8)	2.1789(8)	1.9109

consequently, also the local critical stress values. The global critical stress values for the analysed type of intermediate stiffeners remain virtually unchanged because of small variations in the moment of inertia of the cross-section.

Columns reinforced with intermediate stiffeners may show two local minima for two different local buckling modes (Fig. 8(a) and (b)). The first minimum refers to the smaller number of half-waves m ($m = 7$) and the second one to the greater number of half-waves ($m \approx 51$) as compared with the column without reinforcement. In particular cases the values of these minima for local buckling modes can be almost equal. Each minimum, however, corresponds to a different local buckling mode. Special attention should be paid to the fact that critical stress values referring to the second minimum are nearly equal for both local modes. The theory presented here enables to carry out an analysis of all buckling modes for intermediate stiffeners of different shapes and flexural rigidities. This can help in their rational designing (for more detailed analysis see papers by Kolakowski and Teter, 1995a and Teter and Kolakowski, 1996).

Regarding the global stability, a less favourable case is bevelled corners which reduce the moment of inertia of the cross-section to a greater extent than intermediate stiffeners.

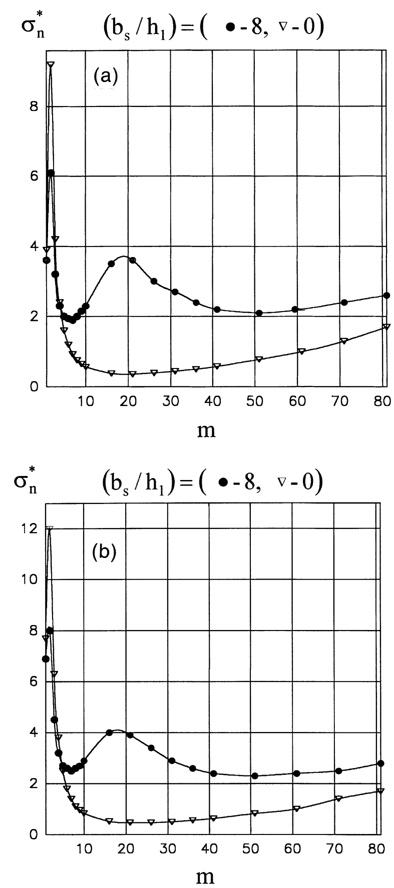

Fig. 8. (a) Dimensionless stress σ_r^* vs the number of half-waves m for uniform compression column ($\kappa = 1$) with cross-section presented in Fig. 3(d). (b) Dimensionless stress σ_r^* vs the number of half-waves m for compressed eccentrically column ($\kappa = 0$) with cross-section presented in Fig. 3(d).

Detailed numerical calculations aiming at the determination of the load carrying capacity of these structures (Fig. 3(d)) with the following imperfections assumed $\bar{\zeta}_1 = | 1.0 |$, $\bar{\zeta}_r = | 0.2 |$ (where $r = 2, \ldots J$) are carried out.

Table 4 present the values of the dimensionless critical stresses, σ_r^*, (the corresponding numbers of half-waves, m are given in parentheses) and the load carrying capacity to the minimum critical stress ratios, $\sigma_{\rm s}^*/\sigma_{\rm m}^*$, for some possible combinations of buckling modes.

The lowest values of stresses $\sigma_{\rm s}^*/\sigma_{\rm m}^*$ for both cases of the compression (i.e. case 4 for $\kappa = 1$ and case 9 for $\kappa = 0$) have been found in the 5-mode approach: the global mode, the local antisymmetric mode ($m \approx 51$) corresponding to the second local minimum, the secondary local symmetric mode corresponding to the latter and two local symmetric modes corresponding to the mode triggered by the global one and having the number of half-waves of two last modes ($m \pm 2$) (according to what is suggested by Byskov, 1987). The five-mode approach gives the limit stress lower nearly 10% than the three-mode approach.

Results obtained for centre intermediate V-stiffeners are analogous to those for C-stiffeners.

The calculations are carried out for a beam-column of an open cross-section reinforced with V-shaped intermediate stiffeners of the following geometrical dimensions (Fig. 9):

$$b_1/b_2 = 2.0; \quad h_1/h_2 = 1.0; \quad l/b_1 = 8; \quad b_1/h_1 = 50; \quad \nu = 0.3$$

and for the V-stiffeners:

$$b_s/h_1 = \{0, 4\}.$$

Figs. 10 and 11 present the dimensionless critical stress, σ_r^*, as a function of the number of half-waves m for $\kappa = 1$ and for $\kappa = 0$, respectively. As a comparison, the results are shown as obtained for a 'smooth' beam-column (that is, $b_{\rm s}/h_1 = 0$, Figs. 10(0) and 11(0)). For the compressed channel section without an intermediate stiffener, the ratio of the flexural–torsional–distortional (primary global) stress to the primary local stress is found here as equal to 2.29 and the ratio of the flexural–distortional (secondary global) stress to the primary local stress is determined as equal to 3.40.

Reinforcing the above compressed channel section with V-shaped intermediate stiffeners causes an increase in the values of the local critical stresses while the values of the global critical stresses do not increase significantly (by approx. 10%) (Fig. 10). The introduction of intermediate stiffeners increases the flexural rigidity of plate elements and the local buckling stress. In these cases the webs are the elements responsible for the local stability loss.

In the case analysed the flexural–torsional buckling precedes the purely flexural one.

Table 4
Load-carrying capacity $\sigma_{\rm s}^*/\sigma_{\rm m}^*$ for beam-column with cross-section presented in Fig. 3(d) with the imperfections $\bar{\zeta}_1 = | 1.0 |$, $\bar{\zeta}_r = | 0.2 |$ (where $r = 2, \ldots J$)

	κ	σ_1^*	σ_2^*	σ_3^*	σ_4^*	σ_5^*	$\sigma_{\rm s}^*/\sigma_{\rm m}^*$
1	1	3.5869(1)	1.9345(7)	2.7215(7)			0.9052
2	1	3.5869(1)	2.1105(51)	2.1146(51)			0.6302
3	1	3.5869(1)	1.9345(7)	2.7215(7)	2.0448(5)	2.1460(9)	0.8833
4	1	3.5869(1)	2.1105(51)	2.1146(51)	2.1146(49)	2.1132(53)	0.5576
5	1	3.5869(1)	1.9345(7)	2.7215(7)	2.1146(51)	2.1146(51)	0.6812
6	0	6.8745(1)	2.3417(7)	6.1912(7)			0.8470
7	0	6.8745(1)	2.2779(52)	3.4132(52)			0.9751
8	0	6.8745(1)	2.5417(7)	6.1912(7)	2.7593(5)	2.7202(9)	0.6566
9	0	6.8745(1)	2.2779(52)	3.4132(52)	2.2828(50)	2.2800(54)	0.6293
10	0	6.8745(1)	2.5417(7)	6.1912(7)	2.2779(52)	3.4132(52)	0.9017

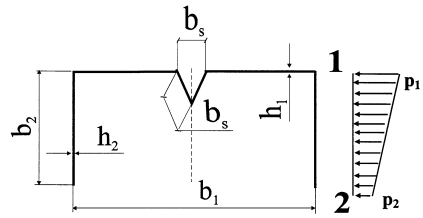

Fig. 9. Channel cross-section.

Fig. 11 shows the dependences of the lowest dimensionless critical stresses, σ_r^*, for beam-columns subjected to the eccentric compression ($\kappa = 0$). In the case of a column without an intermediate stiffener (Fig. 9), the ratio of the global (flexural–torsional–distortional) stress to the local stress is 2.52 while the ratio of the flexural–distortional stress to the local stress is 2.55. In the case of the channel section under discussion the critical stresses rise significantly because of a considerable increase in the stability factors of the flange compressed eccentrically which determine the stability loss.

Table 5 presents the number of half-waves, m, the values of the dimensionless critical stresses, σ_r^*, the ratio of the limit load capacity to the minimum critical stress for the first σ_{s1}^*/σ_m^* and the second σ_{s2}^*/σ_m^* non-linear approximations at the imperfections $\bar{\zeta}_g = |\,1.0\,|$, $\bar{\zeta}_1 = |\,1.0\,|$ and for some possible combinations of buckling modes. The following code has been used: g—for the primary or the secondary global buckling mode ($m = 1$), l—for the local buckling mode ($m > 1$).

In the case of the eccentric compression the global stress values are significantly higher than under the uniform compression while the limit stress values, σ_{s2}^*/σ_m^* are slightly higher (compare cases 1–6, 8, 9–13, 15 in Table 5). This means that the imperfection sensitivity increases together with the eccentricity of the compressive force.

Attention should be paid to the proper selection of local buckling modes—compare cases 7 and 14 in Table 5 (for a more detailed analysis see papers by Kolakowski, 1989a; Teter and Kolakowski, 1996). This can be accomplished only by means of a non-linear analysis.

These data allow us to conclude that the interaction of the two global buckling modes with local modes: the minimum primary symmetric and the secondary antisymmetric ones and two local symmetric ones at ($m \pm 2$) gives the lowest values of the limit stresses σ_{s2}^*/σ_m^*.

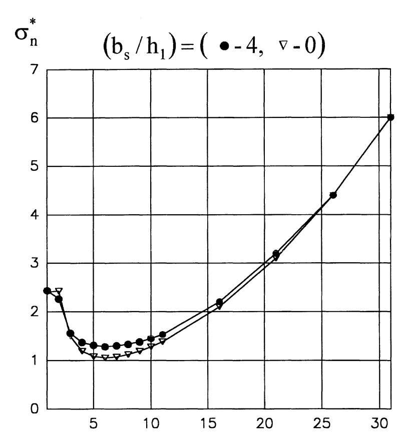

Fig. 10. Dimensionless stress σ_r^* vs the number of half-waves m for uniform compression channel ($\kappa = 1$) presented in Fig. 9.

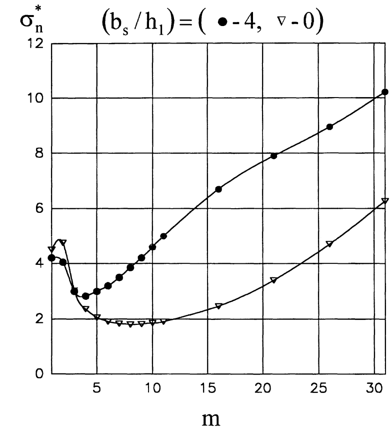

Fig. 11. Dimensionless stress σ_r^* vs the number of half-waves m for compressed eccentrically channel ($\kappa = 0$) presented in Fig. 9.

Results obtained for intermediate C-stiffeners analogous with those for V-stiffeners.

Owing to a good separation of the global modes from the minimum primary local mode this coupled buckling analysis should be carried out in terms of the second order non-linear approximation. In reality, the second order approximation caused a decrease in the range of imperfection sensitivity and allows a proper evaluation of the load carrying capacity.

5. Conclusions

In the case the global stresses exceed the minimum local stress it is possible to attain the load carrying capacity higher than the minimum local stress value for sufficiently small imperfections.

Table 5
Load-carrying capacity σ_s^*/σ_m^* for channel presented in Fig. 9 with the imperfections $\bar{\zeta}_1 =| 1.0 |$, $\bar{\zeta}_l =| 0.2 |$, where the code has been used: g—for the primary or the secondary global buckling mode ($m = 1$), l—for the local buckling mode ($m > 1$)

	κ	σ_1^*	σ_2^*	σ_3^*	σ_4^*	σ_5^*	σ_6^*	σ_{s1}^*/σ_m^*	σ_{s2}^*/σ_m^*
1	1	2.4319(1)	3.2848(1)	1.2870(6)				0.1716	1.0155
2	1	2.4319(1)	3.2848(1)	1.4525(6)				0.1558	0.9159
3	1	2.4319(1)	1.2870(6)	1.4525(6)				0.2029	1.0422
4	1	3.2848(1)	1.2870(6)	1.4525(6)				0.2236	0.7369
5	1	2.4319(1)	3.2848(1)	1.2870(6)	1.4525(6)			0.2031	0.6164
6	1	2.4319(1)	1.2870(6)	1.4525(6)	1.3679(4)	1.3279(8)		0.2187	0.7325
7	1	3.2848(1)	1.2870(6)	1.4525(6)	1.3679(4)	1.3279(8)		0.2235	0.5574
8	1	2.4319(1)	3.2848(1)	1.2870(6)	1.4521(6)	1.3679(4)	1.3279(8)	0.1263	0.5156
9	0	4.1957(1)	4.5715(1)	2.8337(4)				0.1285	0.9519
10	0	4.1957(1)	2.8337(4)	7.8726(4)				0.1853	0.8474
11	0	4.5715(1)	2.8337(4)	7.8726(4)				0.1980	1.1596
12	0	4.1957(1)	4.5715(1)	2.8337(4)	7.8724(4)			0.1853	0.7359
13	0	4.1957(1)	2.8337(4)	7.8726(4)	4.0453(2)	3.1925(6)		0.1767	0.7338
14	0	4.5715(1)	2.8337(4)	7.8726(4)	4.0453(2)	3.1925(6)		0.1946	1.1514
15	0	4.1957(1)	4.5715(1)	2.8337(4)	7.8724(4)	4.0457(2)	3.1925(6)	0.1019	0.6284

The applied method describing the buckling of thin-walled structures from global to local instability can be easily adopted in the computer-aided system, CAD/CAM.

The interactive buckling analysis of thin-walled beam-columns with an intermediate stiffener or/and variable thickness under axial compression and a constant bending moment carried out by means of the transition matrix method has been presented. All global and local modes are described by the plate theory. Intermediate stiffeners are found to exert a strong influence on the local buckling modes. Numerical calculations prove that the mixed buckling mode must be taken into account in the coupled analysis.

Appendix A

The kinematical and statical continuity conditions at the junctions of adjacent plates may be written in the form:

$$u_{i+1}\,|^{-} = u_i\,|^{+}\,,$$

$$w_{i+1}\,|^{-} = w_i\,|^{+}\,\cos(\varphi) - v_i\,|^{+}\,\sin(\varphi),$$

$$v_{i+1}\,|^{-} = w_i\,|^{+}\,\sin(\varphi) + v_i\,|^{+}\,\cos(\varphi),$$

$$w_{i+1,\,y}\,|^{-} = w_{i,\,y}\,|^{+}\,,$$

$$M_{(i+1)y}\,|^{-} = M_{iy}\,|^{+}\,,$$

$$N_{(i+1)y}\,|^{-} - N_{iy}\,|^{+}\,\cos(\varphi) - Q^{*}_{iy}\,|^{+}\,\sin(\varphi) = 0,$$

$$Q^{*}_{(i+1)y}\,|^{+} + N_{iy}\,|^{+}\,\sin(\varphi) - Q^{*}_{iy}\,|^{+}\,\cos(\varphi) = 0,$$

$$N^{*}_{(i+1)xy}\,|^{-} = N^{*}_{ixy}\,|^{+}\,, \tag{12}$$

where

$$N^{*}_{ixy} = N_{ixy} + N_{iy}u_{i,\,y}$$

$$Q^{*}_{iy} = N_{iy}w_{i,\,y} + N_{ixy}w_{i,\,x} + M_{iy,\,y} + 2M_{ixy,\,x}$$

$$\varphi \equiv \varphi_{i;i+1}. \tag{13}$$

The boundary conditions referring to the simply supported beam-columns at their both ends, i.e. $x = 0$ and $x = l$ are assumed to be:

$$\sum_i \frac{1}{b_i}\int_0^{b_i} N_{ix}(x_i = 0,\, y_i)\,\mathrm{d}y_i = \sum_i \frac{1}{b_i}\int_0^{b_i} N_{ix}(x_i = l,\, y_i)\,\mathrm{d}y_i = \sum_i N^{(0)}_{ix},$$

$$v_i(x_i = 0, y_i) = v_i(x_i = l, y_i) = 0,$$

$$w_i(x_i = 0, y_i) = w_i(x_i = l, y_i) = 0,$$

$$M_{iy}(x_i = 0, y_i) = M_{iy}(x_i = l, y_i) = 0. \tag{14}$$

Appendix B

The conditions resulting from the variational principle for two longitudinal edges, for which a relation between the state vectors is derived using the modified transition matrix method, may be written in the form:

$$\int (N_{iy})\delta v_i \, \mathrm{d}x_i \, |_{y_i=\text{const}} = 0;$$

$$\int N^*_{ixy}\delta u_i \, \mathrm{d}x_i \, |_{y_i=\text{const}} = \int (N_{ixy} + N_{iy}u_{i,\,y})\delta u_i \, \mathrm{d}x_i \, |_{y_i=\text{const}} = 0;$$

$$\int (M_{iy})\delta w_{i,\,y} \, \mathrm{d}x_i \, |_{y_i=\text{const}} = 0;$$

$$\int Q^*_{iy}\delta w_i \, \mathrm{d}x_i \, |_{y_i=\text{const}} = \int (M_{iy,\,y} + 2M_{ixy,\,x} + N_{iy}w_{i,\,y} + N_{ixy}w_{i,\,x})\delta w_i \, \mathrm{d}x_i \, |_{y_i=\text{const}} = 0. \tag{15}$$

References

Bernard, E.S., Bridge, R.Q., Hancock, G.J., 1993. Tests of profiled steel decks with V-stiffeners. J. Struct. Engineering 119 (8), 2277–2293.
Biderman, B.L., 1977 (in Russian). In: Mechanics of Thin-walled Structures—Statics. Mashinostroenie, Moscou, p. 488 (in Russian).
Bilstein, W., 1974. Beitrag zur Berechnung vorverformter mit diskreten Laengssteifen ausgesteifter, ausschliesslich in Laengsrichtung belasteter Rechteckplatten nach der nichtlinearen Beultheorie. Der Stahlbau, Heft 7 and Heft 9, pp. 193–201; pp. 276–282.
Byskov, E., 1987. Elastic buckling problem with infinitely many local modes. Mechanics of Structures and Machines 15 (4), 413–435.
Byskov, E., Hutchinson, J.W., 1977. Mode interaction in axially stiffened cylindrical shells. AIAA J. 15 (7), 941–948.
Camotim, D., Prola, I.C., 1996. On the stability of thin-walled columns with Z, S and sigma sections. In: Proceedings of the Second International Conference on Coupled Instability in Metal Structures, Imperial Press College, pp. 149–156.
Cox, H.L., Riddell, J.R., 1949. Buckling of a longitudinal stiffened panel. Aer. Quarterly 1.
Desmond, T.P., 1977. The behaviour and strength of thin-walled compression members with longitudinal stiffeners. Dept. Struct. Engng Report No.369, Cornell University, USA.
Dubina, D., 1996. Coupled instabilities in bar members—general report. In: Proceedings of the Second International Conference on Coupled Instability in Metal Structures, Imperial Press College, pp. 119–132.
Höglund, T., 1978. Design of Trapezoidal Sheeting Provided with Stiffeners in the Flanges and Webs. Manus, Stockholm, Sweden.
Hoon, K.H., Rhodes, J., Seah, L.K., 1993. Tests on intermediately stiffened plate elements and beam compression elements. Thin-Walled Structures 16, 111–143.

Kasagi, A., Sridharan, S., 1995. Modal interaction in composite cylinders under hydrostatic pressure. Int. J. Solids Structures 32 (10), 1349–1369.

Koiter, W.T., 1976. General theory of mode interaction in stiffened plate and shell structures; WTHD Report 590, Delft, p. 41.

Koiter, W.T., Pignataro, M., 1976. An alternative approach to the interaction between local and overall buckling in stiffened panels. In: Buckling of Structures/Proceedings of the IUTAM Symposium, Cambridge, 1974, pp. 133–148.

Koiter, W.T., van der Neut, A., 1980. Interaction between local and overall buckling of stiffened compression panels; In: Thin-Walled Structures, (ed. J. Rhodes and A. G. Walker), Granada, St. Albans, part I, pp. 51–56, part II, pp. 66–86.

Kolakowski, Z., 1993a. Interactive buckling of thin-walled beams with open and closed cross-sections. Thin-Walled Structures 15, 159–183.

Kolakowski, Z., 1993b. Influence of modification of boundary conditions on load carrying capacity in thin-walled columns in the second order approximation. Int. J. Solids Structures 30 (19), 2597–2609.

Kolakowski, Z., 1989a. Interactive buckling of thin-walled beams with open and closed cross-section. Engineering Transactions 37 (2), 375–397.

Kolakowski, Z., 1989b. Mode interaction in wide plate with angle section longitudinal stiffeners under compression. Engineering Transactions 37 (1), 117–135.

Kolakowski, Z., 1989c. Some thougths on mode interaction in thin-walled columns under uniform compression. Thin-Walled Structures 7, 23–35.

Kolakowski, Z., 1987a. Mode interaction in thin-walled trapezoidal column under uniform compression. Thin-Walled Structures 5, 329–342.

Kolakowski, Z., 1987b. Mode interaction in wide plate with closed section longitudinal stiffeners under compression. Engineering Transactions 35 (4), 591–609.

Kolakowski, Z., Teter, A., 1995a. Interactive buckling of thin-walled closed elastic column-beams with intermediate stiffeners. Int. J. Solids Structures 32 (11), 1501–1516.

Kolakowski, Z., Teter, A., 1995b. Influence of local post-buckling behaviour on bending of thin-walled elastic beams with central intermediate stiffeners. Engineering Transactions 43 (3), 383–396.

Kolakowski, Z., Kowal-Michalska, K., Kedziora, S., 1997. Determination of inelastic stability of thin-walled isotropic columns using elastic orthotropic plate equations. Int. J. Mechanics and Mechanical Engineering 1 (1), 79–100.

Konig, L., 1978. Transversely loaded thin-walled C-shaped panels with intermediate stiffeners. Document D7: Swedish Council for Building Research, Sweden.

Krolak, M. (Ed.), 1990. Post-buckling Behaviour and Load Carrying Capacity of Thin-walled Plate Girders. PWN, Polish Scientific Publishers, Warsaw-Lodz, p. 553.

Manevich, A.I., 1988. Interactive buckling of stiffened plate under compression. Mekhanika Tverdogo Tela 5, 152–159 (in Russian).

Manevich, A.I., 1985. Stability of shells and plates with T-section stiffeners. Stroitel'naya Mekhanika i Raschet Sooruzhenii 2, 34–38 (in Russian).

Manevich, A.I., Kolakowski, Z., 1996. Influence of local postbuckling behaviour on bending of thin-walled beams. Thin-Walled Structures 25 (3), 219–230.

Moellmann, H., Goltermann, P., 1989. Interactive buckling in thin-walled beams; Part I: Theory; Part II: Applications. Int. J. Solids Structures, Vol. 25, No. 7, pp. 715–728 and 729–749.

Pignataro, M., Luongo, A., 1987a. Asymmetric interactive buckling of thin-walled columns with initial imperfection. Thin-Walled Structures 3, 365–386.

Pignataro, M., Luongo, A., 1987b. Multiple interactive buckling of thin-walled members in compression. In: Proceedings of the International Colloquium on Stability of Plate and Shell Structures, Ghent, University Ghent, pp. 235–240.

Pignataro, M., Luongo, A., Rizzi, N., 1985. On the effect of the local overall interaction on the postbuckling of uniformly compressed channels. Thin-Walled Structures 3, 283–321.

Sridharan, S., Ali, M.A., 1986. An improved interactive buckling analysis of thin-walled columns having doubly symmetric sections. Int. J. Solids Structures 22 (4), 429–443.

Sridharan, S., Ali, M.A., 1985. Interactive buckling in thin-walled beam-columns. J. Engng Mech. ASCE 111 (12), 1470–1486.

Sridharan, S., Peng, M.H., 1989. Performance of axially compressed stiffened panels. Int. J. Solids and Structures 25 (8), 879–899.

Teter, A., Kolakowski, Z., 1996. Interactive buckling of thin-walled open elastic beam-columns with intermediate stiffeners. Int. J. Solids Structures 33 (3), 315–330.

Timoshenko, S.P., 1921. Tber die Stabilitat versteifter Platten. Der Eisenbau 12, 147–163.

Unger, B., 1969. Elastisches Kippen von beliebig gelagerten und aufgehaengten Durchlauftraegern mit einfachsymmetrischen, in Traegerachse veraenderlichem Querschnitt und einer Abwandlung des Reduktionsverfahrens als Loesungsmethode; Dissertation D17, Darmstadt.